Published in final edited form as:
Transl Res. 2014 July ; 164(1): 70–83. doi:10.1016/j.trsl.2014.03.007.

Epim$^{-/-}$ mice are partially protected from acute colitis via decreased IL-6 signaling

Anisa Shaker, MD[*], **Matthew Gargus, BS**[*], **Julie Fink**[#], **Jana Binkley, BS**[#], **Isra Darwech, MS**[#], **Elzbieta Swietlicki, PhD**[#], **Marc S. Levin, MD**[#], and **Deborah C. Rubin, MD**[#]

[*]Divisions of Gastroenterology and Hepatology at Keck School of Medicine of USC

[#]Divisions of Gastroenterology and Hepatology at Washington University School of Medicine in St. Louis

Abstract

Epimorphin (Epim), a member of the syntaxin family of membrane bound, intracellular vesicle docking proteins, is expressed in intestinal myofibroblasts and macrophages. We have previously demonstrated that *Epim*$^{-/-}$ mice are partially protected from dextran sodium sulfate (DSS)-induced colitis. While IL-6/p-Stat3 signaling has been implicated in the pathogenesis of colitis, the myofibroblast contribution to IL-6 signaling in colitis remains unexplored. Our aim was to investigate the IL-6 pathway in *Epim*$^{-/-}$ mice in the DSS colitis model. Whole colonic tissue, epithelium, and stroma of WT and congenic *Epim*$^{-/-}$ mice treated with 5% DSS for 7 days were analyzed for IL-6 and a downstream effector, p-Stat3, by immunostaining and immunoblot. Colonic myofibroblast and peritoneal macrophage IL-6 secretion were evaluated by ELISA. IL-6 and p-Stat3 expression were decreased in *Epim*$^{-/-}$ vs. WT colon. A relative increase in stromal vs. epithelial p-Stat3 expression was observed in WT mice but not in *Epim*$^{-/-}$ mice. Epim deletion abrogates IL-6 secretion from colonic myofibroblasts treated with IL-1β and decreases IL-6 secretion from peritoneal macrophages in a sub-set of DSS treated mice. Epim deletion inhibits IL-6 secretion most profoundly from colonic myofibroblasts. Distribution of Stat3 activation is altered in DSS treated *Epim*$^{-/-}$ mice. Our findings support the notion that myofibroblasts modulate IL-6/p-Stat3 signaling in DSS treated *Epim*$^{-/-}$ mice.

Keywords

colitis; myofibroblast; epithelial-mesenchymal interactions; IL-6

Reprint requests: Anisa Shaker MD Assistant Professor of Medicine, Keck School of Medicine, University of Southern California, 2011 Zonal Avenue, HMR 810 Los Angeles, CA 90089-0110 P: (323) 442-2084 F: (323) 442-5425.

The authors have no conflicts of interest to declare. All authors have read the journal's policy on disclosure of potential conflicts of interest and the journal's authorship agreement.

Introduction

Ulcerative colitis (UC) and Crohn's disease (CD) are complex, polygenic gastrointestinal inflammatory disorders, that afflict millions of individuals in the United States and worldwide. [1] Accumulating evidence suggests that inflammatory bowel disease (IBD) develops in part as a consequence of a dysregulated immune response to environmental factors/gut microbiota in the genetically susceptible host. [1, 23, 4] Non-traditional innate immune cells such as intestinal sub-epithelial myofibroblasts (ISEMF) have also been implicated in the pathogenesis of IBD.

ISEMFs are mesenchymal cells located subjacent to the basement membrane, at the interface between the epithelium and lamina propria. ISEMFs participate in epithelial-mesenchymal cross-talk and in mediating the immune response via secretion of cytokines, growth factors, and inflammatory mediators. [5] An increase in myofibroblast number has been observed in inflamed UC and CD mucosa. [6] Myofibroblasts in inflamed tissue are characterized by altered proliferation and an increase in secretion of cytokines and extracellular matrix factors. [7] Tissue scarring and fibrosis observed in Crohn's disease has been attributed to the presence of activated myofibroblasts. [7] As extensively reviewed in[8], activated intestinal myofibroblasts produce pro-inflammatory mediators and molecules that may ultimately either down regulate or lead to chronic inflammation. Recent research has also provided insights into the immunosuppressive function of myofibroblasts. Human colonic myofibroblasts, for example, promote the expansion of a subset of regulatory T cells. [9]

These observations are consistent with the active role of myofibroblasts in the pathogenesis of colitis. To further delineate the role of these cells in the pathogenesis of intestinal disorders, we have investigated the role of the unique mesenchymal protein epimorphin (Epim). Epimorphin (Epim) is a member of the syntaxin family of membrane bound, intracellular vesicle docking proteins known as target membrane SNAREs (t-SNARE) that mediate fusion of v-SNARE expressing intracellular secretory vesicles with the plasma membrane. [10] In the gut, Epim is expressed in mesenchymal cells including ISEMFs and has a role in regulating intestinal morphogenesis. [11, 12]

Investigations of the role of Epim in the adult intestine have shown that *Epim*$^{-/-}$ mice are partially protected from dextran sodium sulfate (DSS)-induced acute colitis[13], a well-established chemically induced model of IBD with similarities to ulcerative colitis [1415] frequently used to investigate intestinal injury and repair mechanisms. The mechanisms of protection from DSS induced injury in *Epim*$^{-/-}$ mice are partially a result of improved repair, mediated via an increase in crypt cell proliferation secondary to modulation of Bmp secretion.[13] *Epim*$^{-/-}$ mice also have a markedly reduced dysplastic tumor burden compared to WT mice in the azoxymethane (AOM)/DSS murine model of colitis associated cancer (CAC) [16] mediated in part by a decrease in interleukin (IL)-6 secretion from LPS stimulated intestinal mesenchymal cells. [16] Overall, these findings suggested that in the gut, the effects of Epim are mediated via its functional homology to syntaxin-2 which in turn regulates secretion of signaling factors. [11] The interleukin (IL)-6/signal transducer and activator of transcription-3 (Stat3) signaling pathway has been implicated in the pathogenesis of colitis,

with reports of elevated serum and tissue IL-6 in both IBD and animal models of colitis. IL-6 mediated induction of the transcription factor STAT-3 induces lamina propria T-cell resistance against apoptosis, leading to T cell accumulation and perpetuation of chronic inflammation. [17, 1819]

We were interested, therefore, in exploring the previously unexamined role of Epim deletion on the IL-6 pathway in the acute DSS colitis model. We evaluated IL-6 expression in DSS treated colonic tissue of WT and congenic *Epim*$^{-/-}$ mice. IL-6 signaling was further assessed by evaluating expression of one of its major downstream effectors, p-Stat3, in whole colon, and in enriched colonic epithelium and stroma by immunostaining and immunoblot.

Materials and Methods

Animals

Congenic *Epim*$^{-/-}$ (on a C57BL/6J background) and WT C57Bl/6J male littermates were treated for 7 days with a solution of filtered water containing 5% dextran sodium sulfate (USB). Mice were housed at Washington University School of Medicine barrier facility in a 12-hour light/dark cycle with complete access to food and water. The mice were fed a standard rodent chow diet (PicoLab 20; Purina). Age-matched 8- to 12-week-old *Epim*$^{-/-}$ and WT littermates were used in all experiments. All animal experimentation was approved by the Animal Studies Committee of Washington University School of Medicine where the study was carried out.

Dextran sodium sulfate (DSS) induced colitis

Congenic *Epim*$^{-/-}$ mice (n=27) and WT C57BL/6J mice (n=18) age-matched male littermates were treated for 7 days with a solution of filtered water containing 5% dextran sodium sulfate (DSS) (USB Corporation) in water ad libitum. Daily weights, stool consistency, and rectal bleeding were assessed. Clinical scores were calculated as per Loher et al.[20] Briefly, body weight, fecal blood, and stool consistency were determined at least every other day and given a score ranging from 0 to 4. The overall clinical score was the average of these three scores and ranged from 0 (no activity) to 4 (maximal activity of colitis). We categorized clinical scores < 1 as mild/none; 1-2 as moderate; and > 2 as severe. Animals were sacrificed by CO_2 inhalation on day 8. The colon was removed from its mesentery to the pelvic brim and descending colon was collected for histology and protein analysis. For histologic studies, colons were opened and fixed in 4% formaldehyde (Fisher Scientific International) overnight and transferred to 70% ethanol. They were then cut longitudinally, stabilized in agar and submitted for paraffin embedding and for histological studies. Because DSS induced injury was limited primarily to the descending colon, studies were conducted on this segment of colon unless otherwise specified.

Mucosal injury assessment by Murthy crypt scores

Epim$^{-/-}$ and WT descending colons (n=3 each) were examined under high power (x200) by a two independent observers (AS, JF) blinded to the genotype. The method of crypt scoring by Murthy et al. [21] was used. Briefly, the scoring method was as follows: 0, normal morphology; 1, loss of lower third of the crypt; 2, loss of lower two-thirds of the crypt; 3,

loss of entire crypt but with remaining surface epithelium; and 4, loss of entire glands and epithelium. A field encompassed a 0.07 mm2 circular area and each field was assigned a grade of 0 to 4. The changes were quantitated according to the percentage involvement of the disease process: 1, 1-25%; 2, 26-50%; 3, 51-75%; 4, 76-100% of area examined. Each field was scored with a grade and percentage area of involvement and the product of the two was the crypt score for that field. The crypt scores from all fields in a segment of colon were summed yielding a tissue injury score for that segment of the colon.

Protein isolation and immunoblot

The colon was removed from its mesentery to the pelvic brim and separated into cecum, ascending and descending colon. Protein extraction was performed on sections of descending colon. Tissue was homogenized in 250 μl Tris buffer containing 100 mM Tris-HCL pH 8.0, 100 mM NaCl, 10 mM EDTA, 1% Triton (Fisher Scientific International), 0.1% SDS and protease inhibitor cocktail (Sigma-Aldrich). Then supernatant was sonicated for 30 seconds and centrifuged at 100 × g for 10 minutes to remove unbroken tissue. The pellet was discarded and supernatant was stored at −20°C for use in immunoblot.

Tissue protein concentrations were measured using the Bio-Rad DC protein assay kit. Absorbance was read at 750 nm using a Synergy HT multi-mode microplate reader (BioTek) and data analyzed by Gen5 data analysis software. Aliquots of protein extract (20 μg) were electrophoresed on a 9% SDS polyacrylamide gel and transferred onto a nitrocellulose membrane as per.[16] Immunoblots were incubated with a rabbit polyclonal anti-epimorphin/syntaxin 2 antibody (1:5000; Synaptic Systems), rabbit polyclonal anti-Stat3 antibody (1:2000; Cell Signaling Technology), and mouse monoclonal anti-alpha-tubulin (1:2000; Santa Cruz Biotechnology) to control for differences in total protein loading, followed by a horseradish peroxidase-conjugated anti-IgG antibody (1:5000-1:20,000; Santa Cruz Biotechnology), and developed in chemiluminescent peroxidase substrate (ECL Western Blotting Kit; Amersham Bioscience or SuperSignal West Femto Kit; Fisher Scientific International). Relative abundance of each protein was measured using KODAK analysis of digitized images obtained with an Epson Perfection 1650 scanner using Adobe Photoshop, version CS5.

Epithelial-stromal separation and isolation

Epithelial cells were separated from the non-epithelial compartment utilizing a modification of the EDTA method [22]. Colons were extracted and incubated in tubes of HBSS/5mM EDTA in a 37° C shaker set on 140 RPM for 15 minutes. Tubes were vigorously shaken for 15 seconds. Forceps were used to transfer the tissue segment into a 2nd HBSS/EDTA wash tube and incubation was repeated twice. The 1st HBSS/EDTA was centrifuged at 500G for 5 minutes. The supernatant was removed and 5ml of PBS was added to the remaining fluffy epithelial pellet. These steps were repeated for the 2nd and 3rd wash. All three epithelial collections in PBS were pooled into one tube and centrifuged at 500 G for 10 minutes to remove the supernatant and 100-150 μl cell lysis buffer was added to lyse the pellet and transferred to 1.5ml centrifuge tube (epithelial lysate). 500 μl cell lysis buffer was added to the remaining stromal tissue now stripped of epithelium, homogenized, sonicated for 1 minute, and evaluated for protein by immunoblot or ELISA.

Immunohistochemistry

IL-6 expression in *Epim*$^{-/-}$ and WT descending colon was analyzed using monoclonal mouse anti-IL-6 antibody (1:50; R&D Systems). Sections were deparaffinized with three washes of xylene, hydrated in decreasing grades of ethanol (100%, 95%, 70%, 50%, and dH_2O), and pretreated with Diva DECLOAKER reagent (BIOCARE) for antigen retrieval. Antigen-antibody complexes were detected with biotinylated donkey anti-mouse IgG (1:500; Jackson ImmunoResearch Laboratories) and streptavidin-horseradish peroxidase (1:1000; Jackson ImmunoResearch Laboratories) and diaminobenzidine (BIOCARE). Immunohistochemical analyses of P-STAT3 expression were performed using polyclonal rabbit anti-P-Stat3 antibody (1:50; Cell Signaling Technology). Antigen retrieval was performed with Diva DECLOAKER reagent (BIOCARE); antigen-antibody complexes were detected with biotinylated goat anti-rabbit IgG (1:500; Perkin Elmer) and streptavidin-horseradish peroxidase (1:1000; Jackson ImmunoResearch Laboratories) and diaminobenzidine (BIOCARE).

Immunofluorescensce

Cross sections of formalin fixed, paraffin embedded *Epim*$^{-/-}$ and WT mouse colons were permeabilized with 0.25% triton X-100 (Fisher BP151-100) in PBS following deparaffinization and retrieval of the antigen binding site. Sections were blocked in PBS containing 5% goat serum (Sigma G9023-10ML) for 1 hour prior to adding primary antibody diluted in the same serum containing solution, for overnight incubation at 4°C. Primary antibodies used for α-smooth muscle actin/IL-6 co-staining were mouse anti-α smooth muscle actin (Abcam ab7817, 1:500) and rabbit anti-IL6 (Abcam ab6672, 1:500). Co-stains of rat anti-F4/80 (Abcam ab6640) and rabbit anti-IL6 were diluted at 1:500 and 1:1000, respectively. The next day, sections were washed with PBS followed by incubation with appropriate secondary antibodies: cy2-labeled goat anti-rabbit (Jackson 111-225-114), rhodamine-labeled goat anti-mouse (Jackson 115-297-003) or rhodamine-labeled goat anti-rat (Jackson 112-297-003) at 1:200, for 1 hour at room temperature. Sections were PBS washed before counterstaining with 1ug/ml DAPI in PBS for 1 minute. One last wash with PBS was done before adding fluorescent mounting media (Electron Microscopy Sciences 17985-10) and coverslip.

Peritoneal macrophage isolation from DSS treated mice

Resident peritoneal macrophages were isolated by flushing the peritoneal cavity with cold PBS as described previously [16] from DSS treated WT and *Epim*$^{-/-}$ mice. Cells were counted for viability by trypan blue exclusion; plated (5×105 cells/well) in a 96 well plate in RPMI 1640 media (BioWhittaker) with 2 mM l-glutamine (Life Technologies), 10 mM HEPES, 1 mM sodium pyruvate (BioWhittaker), 50 U/ml penicillin and 50 mg/ml streptomycin (LifeTechnologies), 50 mM 2-ME (Fisher Scientific), and 10% FCS (HyClone); and cultured at 37°C in 5% CO2. After 24 hours, supernatants were collected for measurement of IL-6 and IL-11. ELISA (R&D) was performed per manufacturer's instructions. Results were expressed as pg of cytokine/ml.

Treatment of colonic myofibroblasts with IL-1β

Previously generated WT and *Epim*$^{-/-}$ colonic myofibroblasts[16] (n=3 each) were plated in 6 well plates (100,000 cells/well) and treated with IL-1β (R&D) (0, 1.5, 3, and 100 ng/ml) for 24 hr and then switched to serum free media. Supernatant was collected after 48 hrs and evaluated for IL-6 and IL-11 by ELISA as described above.

Statistics

Data comparing groups is presented as mean ± SEM, and significance was analyzed by 2-tailed Student's t test (Microsoft Excel; Microsoft). P values less than or equal to 0.05 were considered significant.

Results

Epimorphin deletion on a congenic background results in reduced morbidity in acute DSS colitis

A previous study by our lab demonstrated that *Epim*$^{-/-}$ mice on a mixed C57BL/6J 129/SvJ background treated with seven days of 5% dextran-sodium (DSS) had reduced morbidity as measured by clinical scores compared to WT littermates.[13] We began by confirming these findings in congenic *Epim*$^{-/-}$ mice. We treated congenic *Epim*$^{-/-}$ on a C57Bl/6J background (n=18) and WT C57Bl/6J (n=27) littermates with seven days of 5% DSS and similarly observed reduced morbidity in congenic *Epim*$^{-/-}$ versus WT mice. The clinical score accounts for percent body weight loss, rectal bleeding, and stool consistency. Clinical scores were significantly lower in *Epim*$^{-/-}$ mice on days 3 through 6 of DSS treatment compared to WT mice. However, the percentage of body weight loss in congenic *Epim*$^{-/-}$ mice after seven days of DSS was similar to WT littermates (14% versus 15%, p=NS) and by day 7 of treatment, the clinical scores of the two groups was also similar (Figure 1A).

Epimorphin deletion on a congenic background reduces histologic injury in acute DSS colitis

We then wanted to determine whether the decrease in morbidity observed in congenic *Epim*$^{-/-}$ mice translated to histologic protection from injury. In response to treatment with DSS, we observed that *congenic Epim*$^{-/-}$ had reduced histologic evidence of colitis compared to WT mice. Descending colons of *Epim*$^{-/-}$ and WT mice were examined by H&E staining of paraffin embedded sections. WT descending colon demonstrated inflamed, denuded epithelial mucosa with loss of goblet cells (Figure 1B). *Epim*$^{-/-}$ colon demonstrated partially preserved mucosa along with regions of denuded epithelial mucosa (Figure 1C). Sections were then examined under high power (×200) and crypt scoring per Murthy et al [21] was performed to quantify histologic damage. *Epim*$^{-/-}$ mice had a lower crypt damage score in the descending colon than WT mice (Figure 1D). The average Murthy score for WT (n=8) colon was 11.4 and for *Epim*$^{-/-}$ (n=9) colon was 9.1 ($p<0.05$). Thus, both clinical score and histologic injury in response to DSS were reduced in congenic C57Bl6 *Epim*$^{-/-}$ mice compared to WT, although the effects of *Epim* deletion were more modest in this background compared to the protection from colitis reported on the mixed C57Bl6/J/SvJ background.

Epim deletion modulates IL-6 expression

Our previous studies with colonic myofibroblasts[16] demonstrated that secretion of IL-6 was markedly inhibited from LPS treated *Epim*$^{-/-}$ myofibroblasts compared to WT. Therefore, to further explore the mechanisms underlying the partial protection from colitis observed in congenic *Epim*$^{-/-}$ mice, we examined expression of IL-6 in DSS treated *Epim*$^{-/-}$ and WT colon. We performed immunostaining for IL-6 (Figure 2, Supplemental Figure 1). IL-6 expression was predominantly stromal (arrows) in both groups; however, intensity of staining was more prominent in WT (n=5, Figure 2A) compared to *Epim*$^{-/-}$ (n=7, Figure 2B) stroma.

Epim deletion modulates p-Stat3 expression

We then looked at expression of one of the downstream effectors of IL-6 signaling, the nuclear transcription factor p-Stat3 in sections of DSS treated *Epim*$^{-/-}$ and WT colons. We first examined p-Stat3 expression by immunoblot, and measured p-Stat3 band intensity in whole descending colon relative to that of the loading control protein tubulin (Figure 3A). Representative blots of two separate experiments (n=6 WT and n=7 *Epim*$^{-/-}$) are shown. Minimal p-Stat3 expression was detected in whole colonic tissue harvested from untreated WT animals. p-Stat3 was not detected in untreated *Epim*$^{-/-}$ colon. All animals expressed unphosphorylated Stat3. WT mice expressed Epim/syntaxin-2 as expected, while *Epim*$^{-/-}$ mice did not. After treatment with DSS, p-Stat3 expression was blunted in *Epim*$^{-/-}$ compared to WT colon. Quantification of the immunoblot demonstrated that p-Stat3 expression was significantly reduced in the DSS treated *Epim*$^{-/-}$ colon compared to WT colon (Figure 3B). We then evaluated p-Stat3 expression (Figure 4, Supplemental Figure 2) in sections of DSS treated *Epim*$^{-/-}$ and WT colons by immunohistochemistry. Consistent with the findings of the immunoblot, the overall intensity of p-Stat3 nuclear immunostaining (arrows) was reduced in *Epim*$^{-/-}$ (n=4) (Figure 4B, D) versus WT colon (n=6) (Figure 4A, C). P-Stat3 immunostaining was most prominently reduced in the stromal compartment of *Epim*$^{-/-}$; we also noted heterogeneity in epithelial nuclear p-Stat3 immunostaining in *Epim*$^{-/-}$ vs WT colon.

Effect of Epim deletion on p-Stat3 expression in the epithelium versus stroma

We began by performing immunoblots to assess expression of Epim, α-SMA, and tubulin (Figure 5A). Immunoblot for Epim demonstrates its exclusive expression in the non-epithelial compartment, consistent with our assertion that in the gut Epim is a stromal protein. Immunoblot for α-SMA demonstrates that our technique for separating epithelial from non-epithelial cells (lamina propria, submucosa, muscularis propria) was adequate. [22] α-SMA is predominantly expressed in the non-epithelial layer; while tubulin is expressed predominantly in the epithelial layers. The tubulin expressed in some stromal samples reflects spill-over from adjacent over-loaded wells.

We then performed immunoblots for p-Stat3 and Stat3. We observed Stat3 and p-Stat 3 expression in DSS treated WT and *Epim*$^{-/-}$ enriched colonic epithelium and stroma (Figure 5B). Quantification of p-Stat3 expression relative to Stat3 demonstrated that p-Stat3/Stat3 expression was 3.8 fold greater in WT stroma than in WT epithelium of DSS treated mice (p=0.006, Figure 5C). Although a trend toward an increase in p-Stat3/Stat3 expression in

Epim$^{-/-}$ stroma versus epithelium was observed, this difference was not statistically significant (p=0.11). A non-significant trend toward a decrease in p-Stat3/Stat3 in *Epim*$^{-/-}$ vs. WT stroma was observed. p-Stat3/Stat3 was similar in WT and *Epim*$^{-/-}$ epithelium.

We also evaluated IL-6 protein expression in DSS treated WT (n=4) and *Epim*$^{-/-}$ (n=6) descending colon and observed a trend toward a decrease in overall IL-6 expression in *Epim*$^{-/-}$ versus WT DSS treated colon (11.7pg/ml, SEM 7.4 versus 20.6 pg/ml, SEM 10.7, p=0.5).

Epim deletion modulates IL-6 expression in colonic myofibroblasts

We suspected that evaluation of protein lysates for IL-6 was an insensitive method of detecting cellular contributions to the IL-6/p-Stat3 signaling pathway. Therefore, we proceeded to evaluate IL-6 expression in myofibroblasts (Figure 6A-B) and macrophages (Figure 7A-B), two stromal cell populations known to secrete IL-6. We began by performing co-immunostaining for α-SMA and IL-6 in DSS treated WT (n=6) and *Epim*$^{-/-}$ (n=4) descending colon. In WT DSS treated colon, we observed consistent co-expression of IL-6 with α-SMA positive cells and lack of co-expression in areas with less IL-6 expression (Figure 6A, Supplemental Figure 3A, solid and dashed arrows, respectively). In *Epim*$^{-/-}$ colon on the other hand, α-SMA positive cells that did not co-express IL-6 were more frequently observed (Figure 6B, Supplemental Figure 3B, solid versus dash arrows), even in sections with prominent IL-6 expression. Co-immunofluorescence for F4/80 and IL-6 demonstrated similar co-expression of IL-6 in *Epim*$^{-/-}$ versus WT colonic macrophages in DSS treated mice (Figure 7A-B). Immunofluorescent staining again demonstrated an overall decrease in stromal IL-6 expression in *Epim*$^{-/-}$ versus WT colon.

Effect of Epim deletion on colonic myofibroblast secretion of IL-6

We previously demonstrated that Epim deletion markedly inhibits secretion of IL-6 from LPS treated primary cultures of colonic myofibroblasts. In addition, we have previously demonstrated a reduction though not complete inhibition of IL-6 secretion from resident peritoneal macrophages of *naïve Epim*$^{-/-}$ versus WT mice. These findings in combination with our new observation of diminished expression of IL-6 and p-Stat3 in DSS treated *Epim*$^{-/-}$ versus WT colon led us to further investigate the effect of Epim deletion on IL-6 cytokine secretion from myofibroblasts and peritoneal macrophages in the acute DSS model. To mimic the colitis-mediated inflammatory milieu, we treated our previously established primary cultures of colonic myofibroblasts[16] with IL-1β. An increase in IL-1β expression and a pathologic role for IL-1β has been reported in experimental models of colitis, including the DSS model. [15, 23, 24] We observed that in response to 1.5, 3, and 100 ng/ml of IL-1β, WT colonic myofibroblasts secreted 415, 512, and 597 pg/ml of IL-6 respectively ($p<0.05$). IL-6 secretion was not observed in *Epim*$^{-/-}$ colonic myofibroblasts treated with up to 3 ng/ml of IL-1 β and was detected from *Epim*$^{-/-}$ colonic myofibroblasts (16 pg/ml) only after treatment with 100 ng/ml of IL-1β (Figure 8A). We then evaluated secretion of IL-11, a member of the IL-6 cytokine superfamily and another activator of p-Stat3.[25] In response to 100 ng/ml of IL-1β, we observed 108 pg/ml of IL-11 secretion from WT colonic myofibroblasts, five-fold less than the observed IL-6 secretion. IL-11 secretion was not detected in treated *Epim*$^{-/-}$ myofibroblasts (Figure 8B).

Effect of Epim deletion on peritoneal macrophage secretion of IL-6 in DSS treated mice

We then evaluated secretion of IL-6 from peritoneal macrophages from *Epim*$^{-/-}$ (n=12) and WT (n=11) mice after seven days of treatment with DSS. Despite a trend toward a decrease in IL-6 secretion, the effect of Epim deletion on secretion of IL-6 from peritoneal macrophages was not significant (1447 pg/ml, SEM 315 vs. 809 pg/ml, SEM 287, p=0.11) (Figure 9). A wide range of IL-6 secretion was observed from WT (504.5-3294.1 pg/ml) and *Epim*$^{-/-}$ (216.8-3640 pg/ml) mice. We therefore examined IL-6 secretion from mice segregated into groups with similar clinical scores on day 7 of treatment (Figure 10A) and at the time of harvest (Figure 10B). Evaluation of clinical scores on day 7 of DSS treatment (Figure 10A) demonstrated a distribution of scores such that we could group peritoneal macrophage IL-6 secretion according to clinical score severity (minimal < 1; moderate 1-2; and severe >2): one WT mouse and no *Epim*$^{-/-}$ mice had scores < 1; 6/11 WT and 7/12 *Epim*$^{-/-}$ mice had scores 1-2; and 4/11 WT and 4/11 *Epim*$^{-/-}$ mice had scores > 2. Evaluation of IL-6 secretion from WT and *Epim*$^{-/-}$ mice with moderate clinical scores, demonstrated a significant decrease in IL-6 secretion from *Epim*$^{-/-}$ peritoneal macrophages (950.9 pg/ml vs. 346.0 pg/ml, p=0.02). At the time of harvest, the majority of WT (9/11) and *Epim*$^{-/-}$ (7/12) mice had developed severe clinical scores (Figure 10B). IL-6 secretion from *Epim*$^{-/-}$ vs. WT peritoneal macrophages (1112.4 pg/ml vs. 1683.5 pg/ml, respectively) of mice with clinical scores >2 were similar.

Discussion

Although disrupted epithelial-stromal interactions have been implicated in the pathogenesis of colitis, the signaling pathways specific to stromal cells and myofibroblasts remain an ongoing area of investigation. We now show that in congenic DSS-treated *Epim*$^{-/-}$ mice, clinical and histological protection from acute colitis is mediated in part via myofibroblast/stromal modulation of the IL-6/p-Stat3 signaling pathway We have demonstrated a decrease in stromal IL-6 expression and a decrease in expression of its down-stream mediator p-Stat3. We also show a decrease in myofibroblast IL-6 expression and secretion in response to the inflammatory mediator IL-1β. Despite a trend towards a decrease in IL-6 secretion from peritoneal macrophages of DSS treated mice, considerable IL-6 secretion from peritoneal macrophages persisted in the setting of Epim deletion, supporting the crucial contribution of the myofibroblast.

The mechanism of DSS induced injury is not entirely clear. Toxic epithelial injury, alteration in mucin content, macrophage function, and consequent increased exposure to luminal antigens followed by infiltration of polymorphonuclear cells, macrophages, and B and T cells have been proposed as contributors.[15] Animal models of IBD, while not completely reflective of human disease, have been successfully and routinely used to partially interrogate the involved disease pathways in IBD pathogenesis[26]. The DSS model is a well-established chemically induced model of IBD with similarities to ulcerative colitis[15], frequently used to investigate the mechanisms of intestinal injury and repair. [1419]

We have demonstrated that in the acute DSS model Epim deletion results in reduced stromal and myofibroblast expression of IL-6 and its downstream mediator p-Stat3. The predominantly stromal expression of IL-6 in the setting of inflammation has been previously

reported[27] and the IL-6/p-Stat3 pathway has been implicated in the pathophysiology of animal and human colitis.[17, 18281828] IL-6 mediated trans-signaling activation of the transcription factor STAT3 induces the transcription of anti-apoptotic genes bcl-2 and bcl-xl which contribute to T cell resistance against apoptosis, T cell accumulation, and chronic inflammation.[18] Conversely, reduced DSS-induced intestinal inflammation has been reported in IL-6 deficient mice. [29] The effects of the IL-6/STAT3 pathway are cell, tissue, and context specific, however, with distinct roles in homeostasis, inflammation, and tumorigenesis.[30313233] Activation of Stat3 results in regulation of a variety of genes involved in many cellular responses, including proliferation, differentiation, apoptosis, and wound healing. The intestinal activities of p-Stat3 depend on the specific cell types involved. For example, Stat-3 activation in epithelial and myeloid cells mediates mucosa-protective and anti-inflammatory functions, whereas activated Stat-3 in T cells promotes inflammation. [18, 34] To delineate whether the differences in p-Stat3 expression observed in whole colonic tissue were epithelial or stromal, we separated DSS treated WT and *Epim*$^{-/-}$ colon into epithelial and stromal compartments.

Our results suggest that the mechanism by which Epim deletion results in partial protection from DSS-induced colitis is likely multifactorial and is in part a consequence of modulation of stromal and in particular, myofibroblast expression, of the pro-inflammatory cytokine IL-6. Stat3 activation was detected in both stromal and epithelial compartments in DSS treated mice. Epim deletion did not affect the intensity of activated Stat3 expression in the epithelium, whereas it did appear to modulate/hinder stromal Stat3 activation. p-Stat3 immunostaining appeared most consistently reduced in the stromal compartment, with heterogeneity in epithelial nuclear p-Stat3 expression. Consistent with this observation, quantification of p-Stat3 expression in enriched epithelium demonstrated similar p-Stat3 expression in *Epim*$^{-/-}$ and WT mice. Quantification of p-Stat3 in enriched stroma demonstrated a trend towards decreased expression in *Epim*$^{-/-}$ versus WT mice. A more significant difference in stromal p-Stat3 expression may have been obscured by the presence of multiple cells types (lamina propria, submucosa, muscularis propria) in the stromal enriched samples.

Overall, our findings suggest that decreased stromal IL-6 expression in *Epim*$^{-/-}$ mice most profoundly affects stromal p-Stat3 activation and that preserved epithelial p-Stat3 expression in *Epim*$^{-/-}$ mice may be a consequence of other Stat-3 activating cytokines (IL-11, IL-22, IL-27, IL-10) and growth factors (EGF, HGF). [30] Other downstream effectors of IL-6 including Shp2-Ras and phosphatidylinositol-3-kinase (PI3K) may be involved. The relative cell-specific contribution to Stat3 activation in the stromal compartment is likely multifactorial and is a subject of ongoing inquiry.

We have previously demonstrated that Epim deletion abrogates IL-6 secretion from LPS treated colonic myofibroblasts and decreases IL-6 secretion from naïve peritoneal macrophages.[16] We further interrogated the effect of Epim deletion on myofibroblast secretion by treating primary cultures with the inflammatory mediator IL-1β and evaluating secretion of members of the IL-6 cytokine superfamily, IL-6 and IL-11. In WT myofibroblasts, secretion of IL-6 in response to IL-1β was several-fold greater than secretion of IL-11, suggesting that in this model, IL-6 secretion may be a more critical

contributor to pathogenesis. We observed marked inhibition of both of these p-Stat3 activating cytokines from *Epim*$^{-/-}$ colonic myofibroblasts. While diminished p-Stat3 activation in *Epim*$^{-/-}$ mice partially protected from acute colitis raises the possibility of an epiphenomenon associated with an overall decrease in inflammation, modulation of p-Stat3 expression limited to the stroma in *Epim*$^{-/-}$ mice concurrent with a decrease in myofibroblast IL-6 and IL-11 secretion in response to LPS and IL-1β makes this suggestion less likely.

We also investigated the effect of Epim deletion on peritoneal macrophage secretion in the acute DSS model. Our ready detection of IL-6 secretion from peritoneal macrophages harvested from DSS treated animals suggested these cells were in a stimulated state and that further ex-vivo stimulation would not be initially revealing. The less robust effect of Epim deletion on peritoneal macrophage IL-6 secretion was consistent with the similar clinical scores for *Epim*$^{-/-}$ and WT mice at the time of harvest. An effect of Epim deletion on peritoneal macrophage secretion at an earlier time point cannot be ruled out, however. Comparison of IL-6 secretion in mice with clinical scores of moderate severity demonstrated decreased IL-6 secretion from *Epim*$^{-/-}$ versus WT peritoneal macrophages. This observation suggests that the effect of Epim deletion on peritoneal macrophages may be most pronounced early in the course of disease activity. In addition, late in the course of colitis, compensatory mechanisms of IL-6 secretion, such as up-regulation of other syntaxins expressed by macrophages (syntaxin-3, syntaxin-4) [35] may be in effect. Similar immunostaining of IL-6 in colonic macrophages of DSS treated WT and *Epim*$^{-/-}$ colon supports our conclusion that at least by the time of harvest, the effects of Epim deletion are most profound in the myofibroblast. Finally, although peritoneal macrophages are traditionally thought to represent the intestinal environment, are often used in functional studies, and are well-described in the colitis model [36, 37], this population may be different in the un-stimulated/un-treated versus stimulated/DSS-treated animal and may in fact reflect functionally distinct subsets. [38]

A clear understanding of the stromal-mediated pathways in the pathogenesis of intestinal injury and inflammation is paramount. Infiltrating innate immune cells (neutrophils, macrophages, dendritic, and natural killer cells) trigger inflammatory responses via secretion of cytokines. [2] Cytokine imbalance between effector and regulatory T cells in turn contributes to disease pathogenesis. [3] An increase in IL-6 and IL-1β expression has been reported in colonic mucosa of UC and CD patients. [3] These cytokines partially mediate the interactions between immune cells, neighboring mesenchymal and overlying epithelial cells. [2] Our results confirm that myofibroblast cytokine secretion may be contributing to the cross-talk in the inflammatory milieu.

A logical extension of the interesting findings in *Epim*$^{-/-}$ mice in the acute DSS model is evaluation of epimorphin expression in human IBD specimens. Unfortunately, however, characterization of epimorphin expression in inflammatory bowel disease specimens has thus far yielded inconsistent results. One study showed an alteration in the distribution of epimorphin expression in active UC compared to inactive UC, and in active and inactive CD. [39] These investigators observed diminished epimorphin expression in cells surrounding the epithelium, but an overall increase in the number of epimorphin positive cells. Another

study using a different antibody demonstrated no change in epimorphin expression in normal compared to colitis specimens. [40] These inconsistent findings are likely a consequence of differences in the specificity of antibody used to detect epimorphin. More recent studies suggest that consistent detection of this protein may be best achieved by immunostaining on frozen versus paraffin embedded sections.[41]

Overall, little is known about the mechanisms whereby myofibroblasts contribute to ongoing inflammation. It has been suggested that myofibroblasts derived from epithelial to mesenchymal transition (EMT) and/or bone marrow (BM) stem cell migration may be responsible through yet unknown mechanisms. Bone marrow transplant following whole body irradiation in murine models has demonstrated that nearly 60% of pericryptal myofibroblasts at 6 weeks post transplantation are derived from bone marrow.[42] Tissue engraftment and myofibroblast formation increase in the setting of TNBS colitis.[7] Bone marrow derived myofibroblasts have also been observed in transplant patients afflicted with graft versus host disease.[42] We have not addressed whether the *Epim*$^{-/-}$ myofibroblasts participating in protection from DSS colitis are resident, bone-marrow-derived, or a combination thereof. More recently a role for mesenchymal stem cells in sustaining colitis by forming a niche for colitogenic T cells has been reported. [43] Our findings confirm that myofibroblasts are active participants in the inflammatory response and that modulation of their secretory function via Epim deletion has protective effects in the acute DSS model.

In conclusion, in an inflammatory milieu, Epim deletion abrogates IL-6 secretion most profoundly from colonic myofibroblasts, with a variable effect on peritoneal macrophages. The distribution of Stat3 activation is altered in DSS treated *Epim*$^{-/-}$ mice, with a trend toward a decrease in the *Epim*$^{-/-}$ stroma. Our findings support the notion that myofibroblasts modulate IL-6/p-Stat3 signaling in DSS treated *Epim*$^{-/-}$ mice and confirm a role for this stromal protein in the pathogenesis of colitis.

Supplementary Material

Refer to Web version on PubMed Central for supplementary material.

Acknowledgements

Sources of support: NIH/NCI KO8CA153036-01A1, AGA-General Mills Bell Institute of Health and Nutrition Research Scholar Award in Gut Physiology and Health (A Shaker), NIH NIDDK R01 DK46122 and R01DK61216 (D Rubin), NIH/NIDDK DDRCC P30 DK52574 (Wash U), and NIH P30 DK048522, S10 RR022508 (USC)

abbreviations

IBD	inflammatory bowel disease
ISEMF	intestinal sub-epithelial myofibroblast
Epim	epimorphin
DSS	dextran sodium sulfate
IL	interleukin

References

1. Rubin DC, Shaker A, Levin MS. Chronic intestinal inflammation: inflammatory bowel disease and colitis-associated colon cancer. Front Immunol. 2012; 3:107. [PubMed: 22586430]
2. Bouguen G, Chevaux JB, Peyrin-Biroulet L. Recent advances in cytokines: therapeutic implications for inflammatory bowel diseases. World J Gastroenterol. 2011; 17:547–56. [PubMed: 21350703]
3. Sanchez-Munoz F, Dominguez-Lopez A, Yamamoto-Furusho JK. Role of cytokines in inflammatory bowel disease. World J Gastroenterol. 2008; 14:4280–8. [PubMed: 18666314]
4. Salim SY, Soderholm JD. Importance of disrupted intestinal barrier in inflammatory bowel diseases. Inflamm Bowel Dis. 2011; 17:362–81. [PubMed: 20725949]
5. Powell DW, Mifflin RC, Valentich JD, et al. Myofibroblasts. II. Intestinal subepithelial myofibroblasts. Am J Physiol. 1999; 277:C183–201. [PubMed: 10444394]
6. Andoh A, Fujino S, Okuno T, et al. Intestinal subepithelial myofibroblasts in inflammatory bowel diseases. J Gastroenterol. 2002; 37(Suppl 14):33–7. [PubMed: 12572863]
7. Brittan M, Chance V, Elia G, et al. A regenerative role for bone marrow following experimental colitis: contribution to neovasculogenesis and myofibroblasts. Gastroenterology. 2005; 128:1984–95. [PubMed: 15940631]
8. Pinchuk IV, Mifflin RC, Saada JI, et al. Intestinal mesenchymal cells. Curr Gastroenterol Rep. 2010; 12:310–8. [PubMed: 20690004]
9. Pinchuk IV, Beswick EJ, Saada JI, et al. Human colonic myofibroblasts promote expansion of CD4+ CD25high Foxp3+ regulatory T cells. Gastroenterology. 2011; 140:2019–30. [PubMed: 21376048]
10. Rothman JE. Mechanisms of intracellular protein transport. Nature. 1994; 372:55–63. [PubMed: 7969419]
11. Fritsch C, Swietlicki EA, Lefebvre O, et al. Epimorphin expression in intestinal myofibroblasts induces epithelial morphogenesis. J Clin Invest. 2002; 110:1629–41. [PubMed: 12464668]
12. Goyal A, Singh R, Swietlicki EA, et al. Characterization of rat epimorphin/syntaxin 2 expression suggests a role in crypt-villus morphogenesis. Am J Physiol. 1998; 275:G114–24. [PubMed: 9655691]
13. Wang Y, Wang L, Iordanov H, et al. Epimorphin(−/−) mice have increased intestinal growth, decreased susceptibility to dextran sodium sulfate colitis, and impaired spermatogenesis. J Clin Invest. 2006; 116:1535–46. [PubMed: 16710473]
14. Mizoguchi A. Animal models of inflammatory bowel disease. Prog Mol Biol Transl Sci. 2012; 105:263–320. [PubMed: 22137435]
15. Melgar S, Karlsson A, Michaelsson E. Acute colitis induced by dextran sulfate sodium progresses to chronicity in C57BL/6 but not in BALB/c mice: correlation between symptoms and inflammation. Am J Physiol Gastrointest Liver Physiol. 2005; 288:G1328–38. [PubMed: 15637179]
16. Shaker A, Swietlicki EA, Wang L, et al. Epimorphin deletion protects mice from inflammation-induced colon carcinogenesis and alters stem cell niche myofibroblast secretion. J Clin Invest. 2010; 120:2081–93. [PubMed: 20458144]
17. Li Y, Yu C, Zhu WM, et al. Triptolide ameliorates IL-10-deficient mice colitis by mechanisms involving suppression of IL-6/STAT3 signaling pathway and down-regulation of IL-17. Mol Immunol. 2010; 47:2467–74. [PubMed: 20615550]
18. Mudter J, Neurath MF. Il-6 signaling in inflammatory bowel disease: pathophysiological role and clinical relevance. Inflamm Bowel Dis. 2007; 13:1016–23. [PubMed: 17476678]
19. Valatas V, Vakas M, Kolios G. The value of experimental models of colitis in predicting efficacy of biologic therapies for inflammatory bowel diseases. Am J Physiol Gastrointest Liver Physiol. 2013
20. Loher F, Schmall K, Freytag P, et al. The specific type-4 phosphodiesterase inhibitor mesopram alleviates experimental colitis in mice. J Pharmacol Exp Ther. 2003; 305:549–56. [PubMed: 12606674]

21. Murthy SN, Cooper HS, Shim H, et al. Treatment of dextran sulfate sodium-induced murine colitis by intracolonic cyclosporin. Dig Dis Sci. 1993; 38:1722–34. [PubMed: 8359087]
22. Newberry RD, Stenson WF, Lorenz RG. Cyclooxygenase-2-dependent arachidonic acid metabolites are essential modulators of the intestinal immune response to dietary antigen. Nat Med. 1999; 5:900–6. [PubMed: 10426313]
23. Coccia M, Harrison OJ, Schiering C, et al. IL-1beta mediates chronic intestinal inflammation by promoting the accumulation of IL-17A secreting innate lymphoid cells and CD4(+) Th17 cells. J Exp Med. 2012; 209:1595–609. [PubMed: 22891275]
24. Siegmund B, Lehr HA, Fantuzzi G, et al. IL-1 beta -converting enzyme (caspase-1) in intestinal inflammation. Proc Natl Acad Sci U S A. 2001; 98:13249–54. [PubMed: 11606779]
25. Hoang B, Trinh A, Birnbaumer L, et al. Decreased MAPK- and PGE2-dependent IL-11 production in Gialpha2−/− colonic myofibroblasts. Am J Physiol Gastrointest Liver Physiol. 2007; 292:G1511–9. [PubMed: 17332478]
26. Wirtz S, Neurath MF. Mouse models of inflammatory bowel disease. Adv Drug Deliv Rev. 2007; 59:1073–83. [PubMed: 17825455]
27. Hugo HJ, Lebret S, Tomaskovic-Crook E, et al. Contribution of Fibroblast and Mast Cell (Afferent) and Tumor (Efferent) IL-6 Effects within the Tumor Microenvironment. Cancer Microenviron. 2012
28. Lee MJ, Lee JK, Choi JW, et al. Interleukin-6 induces S100A9 expression in colonic epithelial cells through STAT3 activation in experimental ulcerative colitis. PLoS One. 2012; 7:e38801. [PubMed: 22962574]
29. Naito Y, Takagi T, Uchiyama K, et al. Reduced intestinal inflammation induced by dextran sodium sulfate in interleukin-6-deficient mice. Int J Mol Med. 2004; 14:191–6. [PubMed: 15254764]
30. Neufert C, Pickert G, Zheng Y, et al. Activation of epithelial STAT3 regulates intestinal homeostasis. Cell Cycle. 2010; 9:652–5. [PubMed: 20160497]
31. Willson TA, Jurickova I, Collins M, et al. Deletion of Intestinal Epithelial Cell STAT3 Promotes T-Lymphocyte STAT3 Activation and Chronic Colitis Following Acute Dextran Sodium Sulfate Injury in Mice. Inflamm Bowel Dis. 2013; 19:512–25. [PubMed: 23429443]
32. Li N, Grivennikov SI, Karin M. The unholy trinity: inflammation, cytokines, and STAT3 shape the cancer microenvironment. Cancer Cell. 2011; 19:429–31. [PubMed: 21481782]
33. Yu H, Kortylewski M, Pardoll D. Crosstalk between cancer and immune cells: role of STAT3 in the tumour microenvironment. Nat Rev Immunol. 2007; 7:41–51. [PubMed: 17186030]
34. Mudter J, Neurath MF. Apoptosis of T cells and the control of inflammatory bowel disease: therapeutic implications. Gut. 2007; 56:293–303. [PubMed: 16956919]
35. Shukla A, Berglund L, Nielsen LP, et al. Regulated exocytosis in immune function: are SNARE-proteins involved? Respir Med. 2000; 94:10–7. [PubMed: 10714474]
36. Andou A, Hisamatsu T, Okamoto S, et al. Dietary histidine ameliorates murine colitis by inhibition of proinflammatory cytokine production from macrophages. Gastroenterology. 2009; 136:564–74. e2. [PubMed: 19027739]
37. Kure I, Nishiumi S, Nishitani Y, et al. Lipoxin A4 reduces lipopolysaccharide-induced inflammation in macrophages and intestinal epithelial cells through inhibition of NF-{kappa}B activation. J Pharmacol Exp Ther. 2009
38. Ghosn EE, Cassado AA, Govoni GR, et al. Two physically, functionally, and developmentally distinct peritoneal macrophage subsets. Proc Natl Acad Sci U S A. 2010; 107:2568–73. [PubMed: 20133793]
39. Shirasaka T, Iizuka M, Yukawa M, et al. Altered expression of epimorphin in ulcerative colitis. J Gastroenterol Hepatol. 2003; 18:570–7. [PubMed: 12702050]
40. Andoh A, Fujino S, Hirai Y, et al. Epimorphin expression in human colonic myofibroblasts. Int J Mol Med. 2004; 13:57–61. [PubMed: 14654971]
41. Yamada M, Oda T, Higashi K, et al. Involvement of epimorphin in the repair of experimental renal fibrosis in mice. Lab Invest. 2010; 90:867–80. [PubMed: 20195239]
42. Brittan M, Hunt T, Jeffery R, et al. Bone marrow derivation of pericryptal myofibroblasts in the mouse and human small intestine and colon. Gut. 2002; 50:752–7. [PubMed: 12010874]

43. Nemoto Y, Kanai T, Takahara M, et al. Bone marrow-mesenchymal stem cells are a major source of interleukin-7 and sustain colitis by forming the niche for colitogenic CD4 memory T cells. Gut. 2013; 62:1142–52. [PubMed: 23144054]

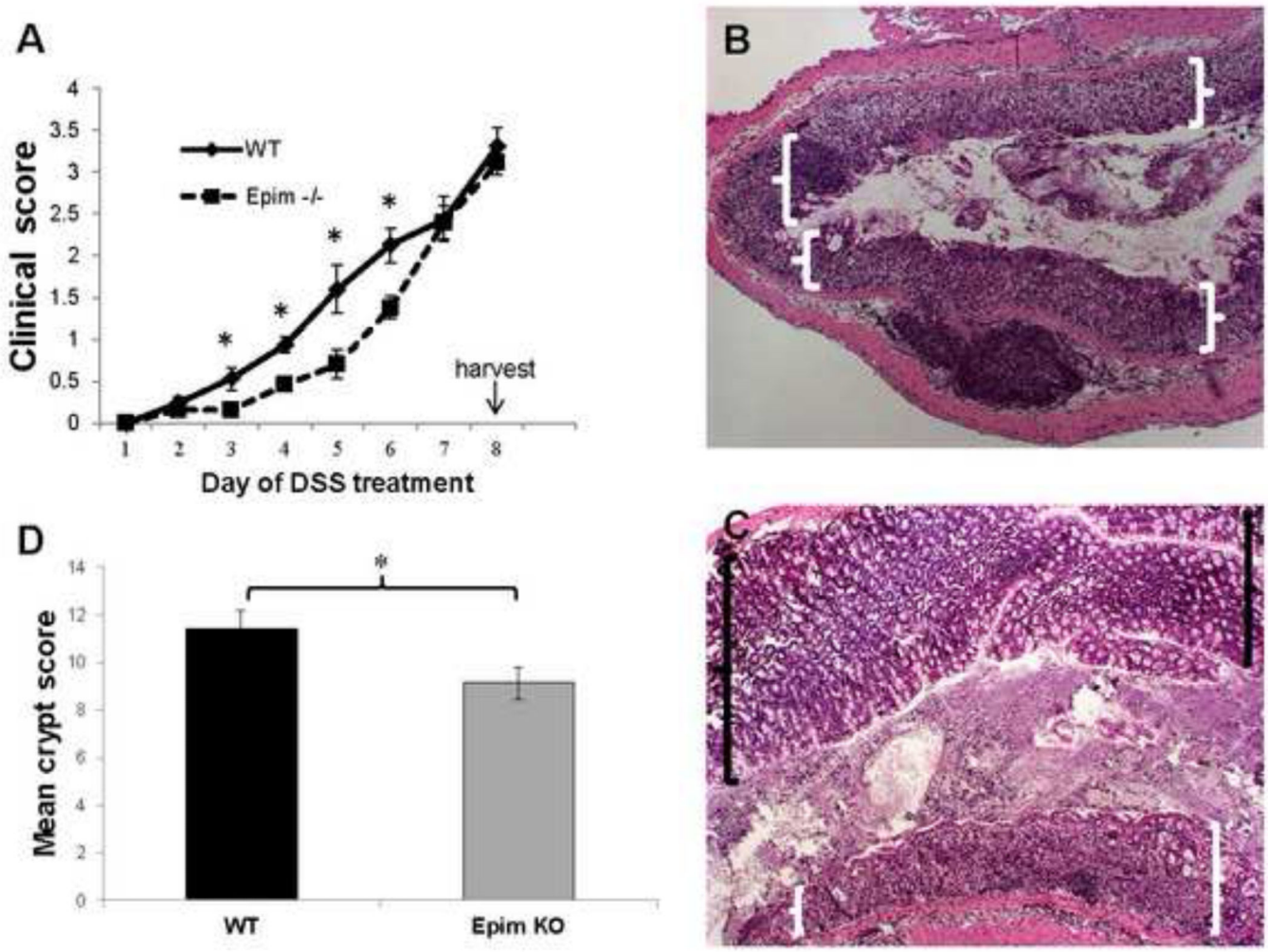

Figure 1. Congenic *Epim*$^{-/-}$ are partially protected from DSS colitis

Epim$^{-/-}$ (on a C57BL/6J background; n=27) and WT C57Bl/6J (n=18) male littermates were treated with 7 days of dextran sodium sulfate (USB corporation). **(A)** *Congenic Epim*$^{-/-}$ mice have reduced clinical colitis scores compared to WT mice in response to treatment with DSS. Percentage body weight loss, fecal blood, stool consistency were evaluated and scored daily as per. [20] The average of these parameters was calculated to determine a clinical score. Clinical signs of colitis defined by a score of ≥0.5 were evident in WT mice starting on Day 2 of DSS. *Epim*$^{-/-}$ did not demonstrate clinical signs of colitis until Day 5. By day 7 the clinical severity of colitis in *Epim*$^{-/-}$ and WT mice was similar. **(B-D)** *Congenic Epim*$^{-/-}$ have less histologic evidence of colitis compared to WT mice in response to treatment with DSS. *Epim*$^{-/-}$ (n=9) and WT (n=8) descending colons were examined by hematoxylin and eosin staining of paraffin embedded sections. Representative sections of WT and *Epim*$^{-/-}$ descending colons at the completion of 7 days of DSS are shown. **(B)** WT descending colon demonstrates entirely denuded epithelial mucosa (white brackets, original magnification, x50). **(C)** *Epim*$^{-/-}$ colon demonstrates partially preserved mucosa (black brackets) along with regions of denuded epithelial mucosa (white brackets, x50). **(D)** Sections were then examined under high power (x200) and crypt scoring per Murthy et al [21]

was performed to quantitate histologic damage. The average Murthy score for WT descending colon (n=8) was 11.4 and for *Epim*$^{-/-}$ (n=9) descending colon 9.1 ($p<0.05$).

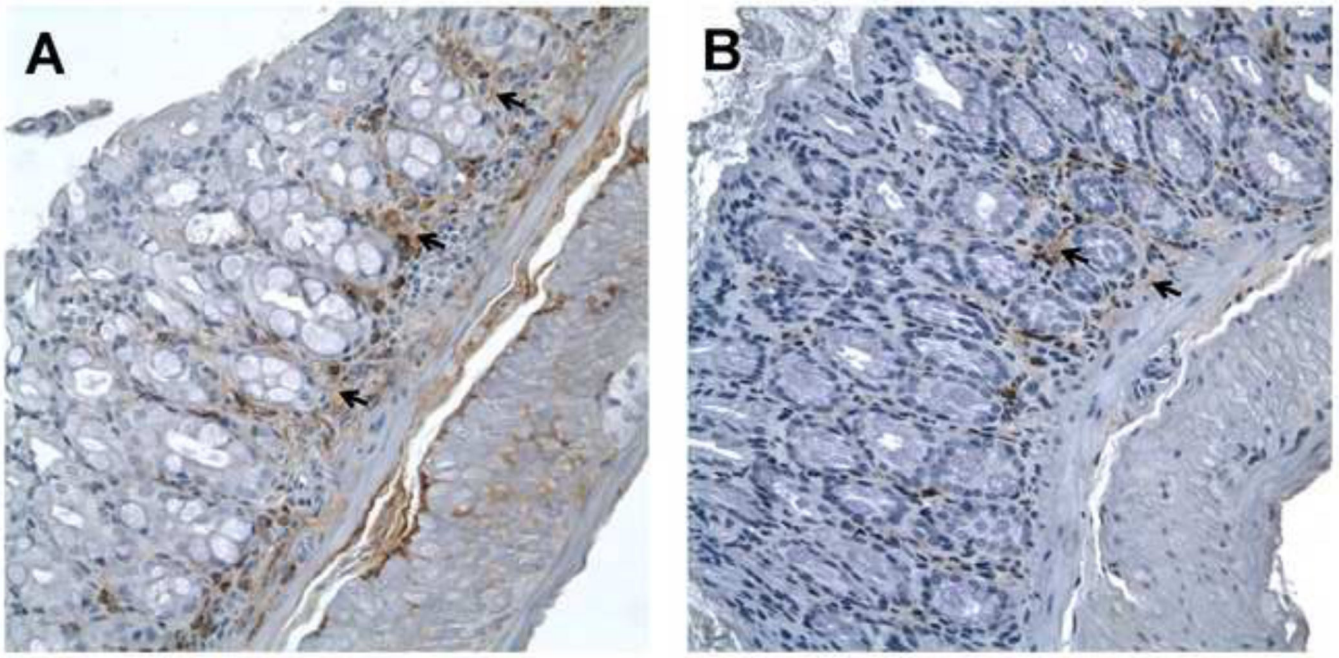

Figure 2. IL-6 expression is decreased in descending colon of *Epim*$^{-/-}$ mice treated with DSS

Representative sections of WT (n=5, **A)** and *Epim*$^{-/-}$ (n=7, **B)** intact descending colons were immunostained with an anti -IL-6 antibody (R&D, 1:50). IL-6 expression is predominantly stromal in WT and *Epim*$^{-/-}$ colon. Intensity of stromal staining is more prominent in WT compared to *Epim*$^{-/-}$ stroma (black arrows). Magnification 400×.

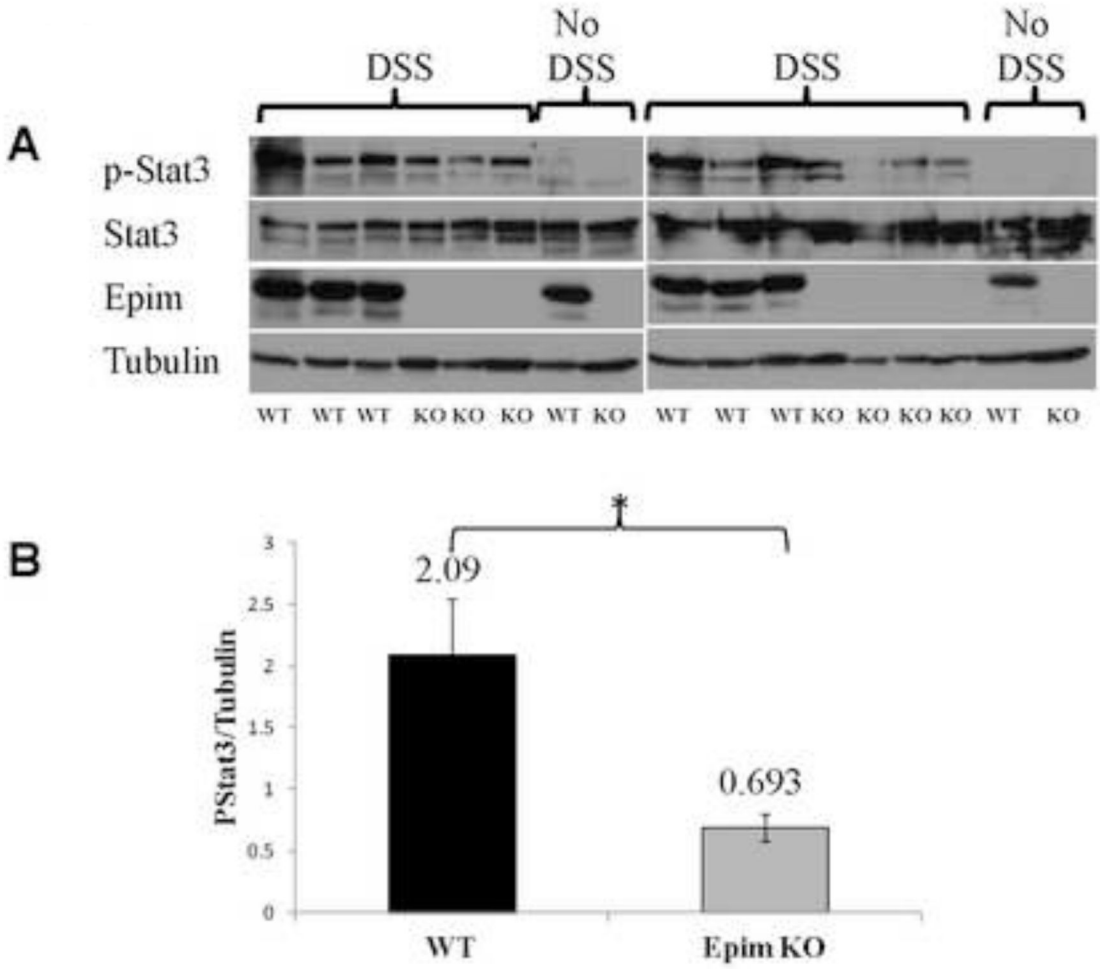

Figure 3. p-Stat3 expression is decreased in *Epim*$^{-/-}$ DSS treated colon

p-Stat3 expression in *Epim*$^{-/-}$ descending colon was examined by immunoblot. Representative blots of two separate experiments are shown (**A**). p-Stat3 band intensity relative to that of the loading protein tubulin was measured. As expected, there is minimal to no p-Stat3 expression in untreated animals. All animals expressed un-phosphorylated Stat3. Only WT mice expressed Epim. The bottom row shows the loading protein tubulin. After treatment with DSS, there is a blunted increase in p-Stat3 expression in *Epim*$^{-/-}$ versus WT colon. (**B**) Quantification of band intensity confirms that p-Stat3 expression remained significantly less in the DSS treated *Epim*$^{-/-}$ (n=7) compared to WT (n=6) colon.

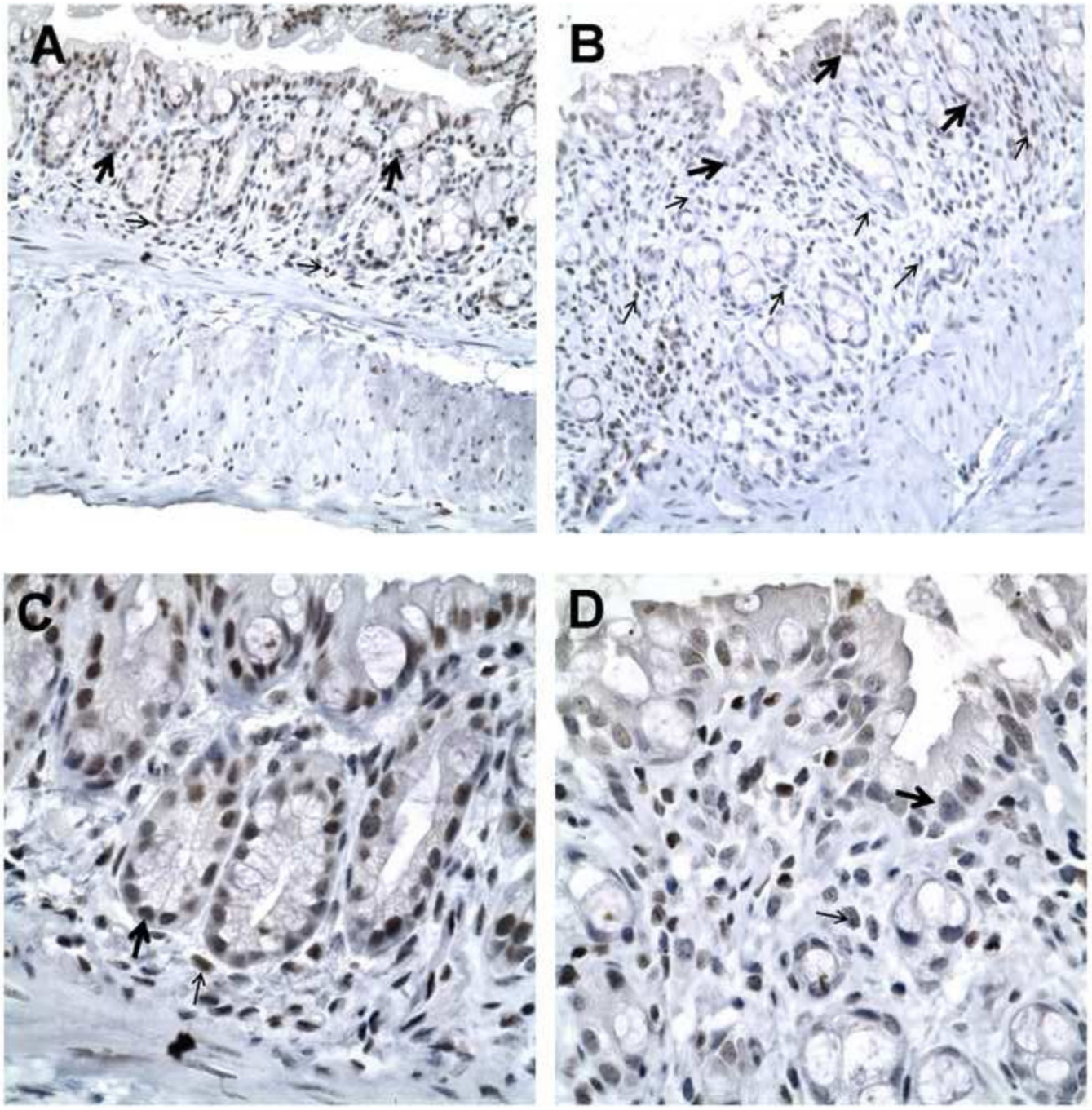

Figure 4. p-Stat3 expression is decreased in *Epim*$^{-/-}$ DSS treated colon

Representative sections of WT (**A, C**) and *Epim*$^{-/-}$ (**B, D**) colon were immunostained with p-Stat3 (Cell Signaling Technology, 1:50). p-Stat3 nuclear staining is evident in epithelial (thick arrows) and stromal (thin arrows) cells in WT (n=4) and *Epim*$^{-/-}$ (n=4) colon. The intensity of p-Stat3 nuclear staining appears less intense in *Epim*$^{-/-}$ compared to WT colon. Magnification A-B 400x; C-D 1000×.

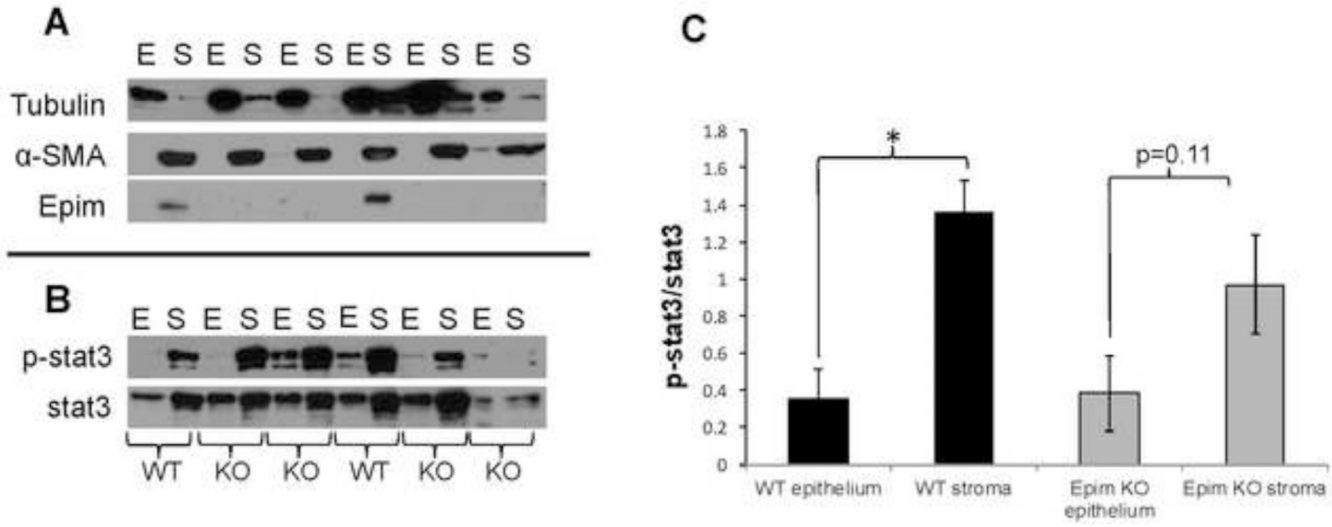

Figure 5. p-Stat3 expression in DSS treated *Epim*$^{-/-}$ and WT epithelial and stromal compartments

(A). Representative immunoblots for Epim, Tubulin, and α-SMA expression in DSS treated *Epim*$^{-/-}$ and WT descending colon are shown. Epim is detected only in the stromal compartment of WT mice. α-SMA is predominantly expressed in the non-epithelial layer; while tubulin is expressed predominantly in the epithelial layers. **(B).** Representative immunoblots for p-Stat3 and Stat3 expressed in epithelial and stromal compartments of WT and *Epim*$^{-/-}$ mice. **(C).** Quantification of p-Stat3 expression in the epithelial versus the stromal compartments of DSS treated WT and *Epim*$^{-/-}$ mice. p-Stat3 normalized to Stat3 demonstrates that in WT colon, p-Stat3 expression is greater in the stromal versus epithelial compartment. In contrast, the difference in p-Stat3 expression in *Epim*$^{-/-}$ stromal versus epithelial compartments was not significant.

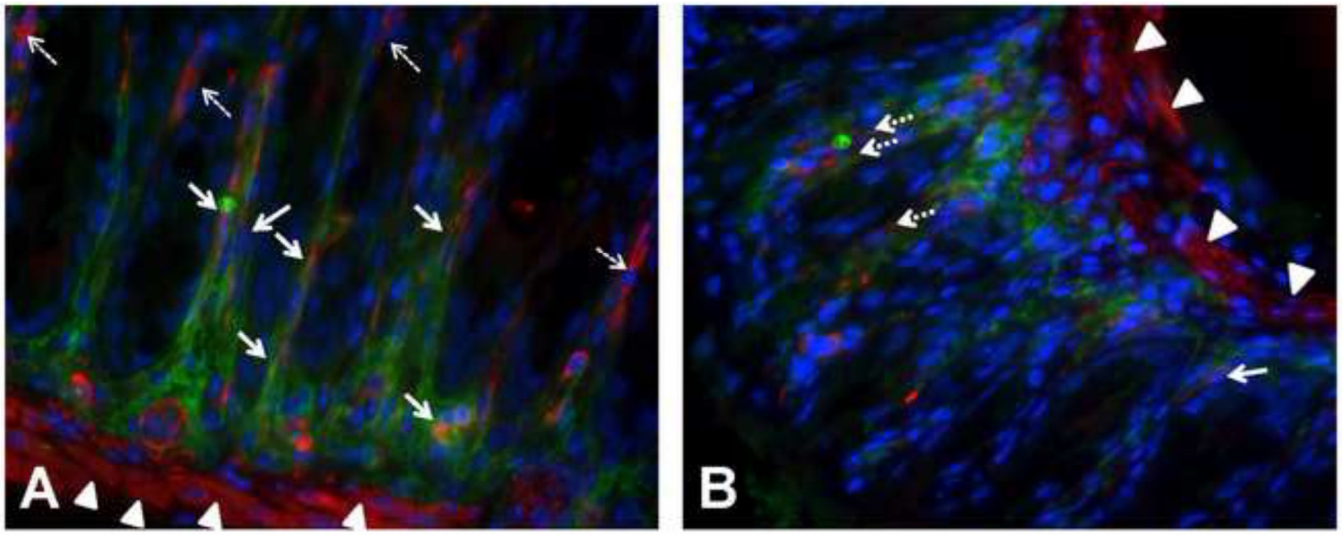

Figure 6. IL-6 expression in colonic myofibroblasts in WT and *Epim*$^{-/-}$ DSS treated colon

Representative sections of formalin fixed paraffin embedded WT (n=5, **A)** and *Epim*$^{-/-}$ (n=4, **B)** intact descending colons were immunostained with rabbit anti -IL-6 (Abcam ab6672, 1:500), and mouse anti-α smooth muscle actin (α-SMA) (Abcam ab7817, 1:500) primary antibodies, followed by rhodamine-labeled (red) goat anti-mouse (Jackson 115-297-003, 1:200) and cy2-labeled (green) goat anti-rabbit (Jackson 111-225-114, 1:200) secondary antibodies, respectively. The muscularis mucosa expresses α-SMA (red, arrow heads). **(A)** Stromal IL-6 (green, cy2) is readily detected in WT DSS treated descending colon. In areas of WT colon with prominent IL-6 expression, co-immunostaining (yellow, orange) of α-SMA and IL-6 is observed in cells lining the crypts. **(B).** There is less intense stromal IL-6 expression (green, cy2) in DSS treated *Epim*$^{-/-}$ versus WT colon. α-SMA expressing cells that do not co-express IL-6 (dashed white arrows) and IL-6 expressing cells that do not co-express α-SMA are more frequently observed in sections of DSS treated *Epim*$^{-/-}$ colon. The muscularis mucosa immunostains for α-SMA and is indicated by arrowheads. Blue is DAPI. Magnification 400× oil.

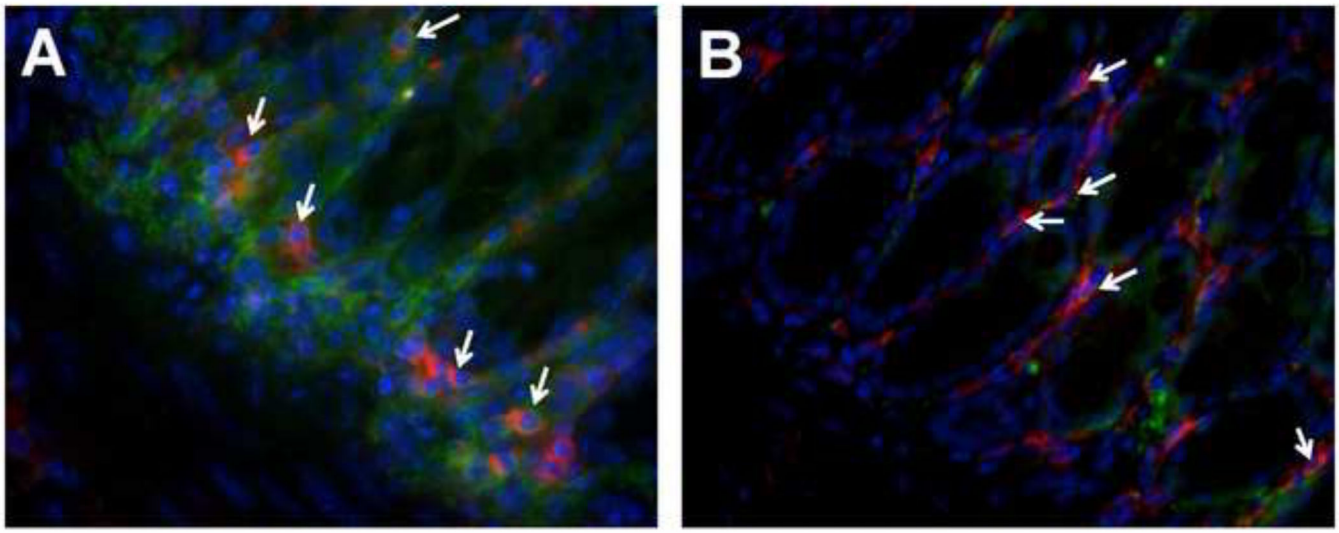

Figure 7. IL-6 expression in colonic macrophages in WT and *Epim*$^{-/-}$ DSS treated colon

Representative sections of formalin fixed paraffin embedded WT (n=5, **A**) and *Epim*$^{-/-}$ (n=4, **B**) Intact descending colons were immunostained with rat anti-F4/80 (Abcam ab6640, 1:500) and rabbit anti-IL6 (Abcam ab6672, 1:500) primary antibodies followed by rhodamine-labeled (red) goat anti-rat (Jackson 112-297-003, 1:1000) and cy2-labeled (green) goat anti-rabbit secondary antibody (Jackson 111-225-114, 1:1000) secondary antibodies respectively. Co-immunofluorescence for F4/80 and IL-6 shows similar co-expression of IL-6 in *Epim*$^{-/-}$ versus WT colonic macrophages in DSS treated mice. Immunofluorescent staining for F4/80 and IL-6 again demonstrates an overall decrease in stromal IL-6 expression in *Epim*$^{-/-}$ versus WT colon. Magnification 400× oil.

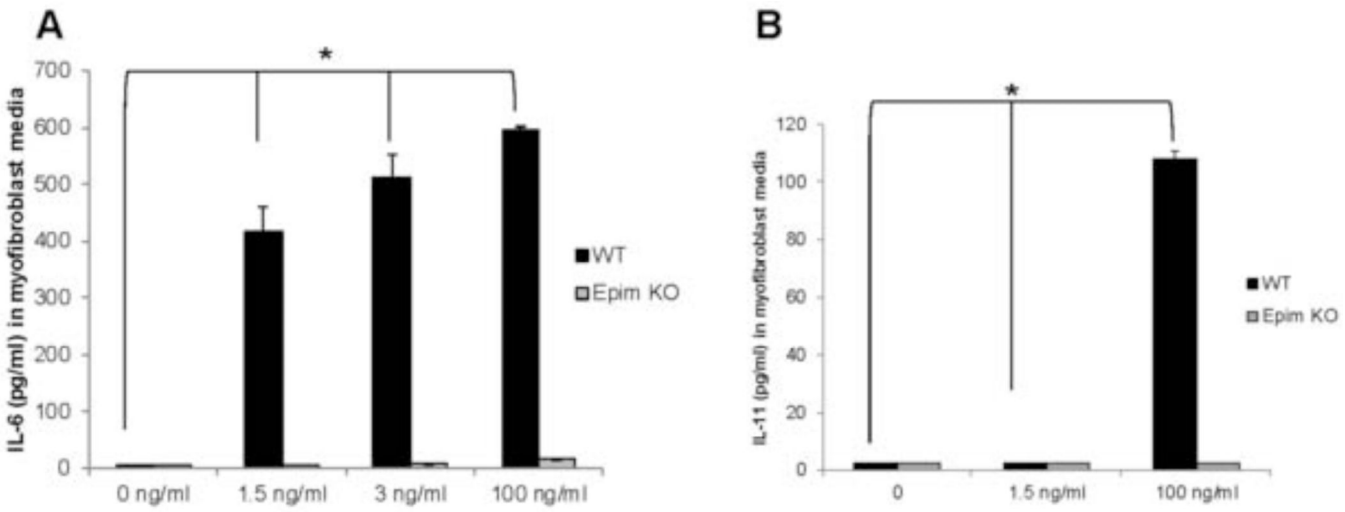

Figure 8. Epim deletion in colonic myofibroblasts treated with IL-1β abrogates secretion of IL-6 family of cytokines

WT and *Epim*$^{-/-}$ myofibroblasts were plated in 6 well plates and treated with IL-1β (1.5, 3, and 100 ng/ml) for 24 hr. Supernatant was collected after 48 hours and IL-6 and IL-11 secretion were evaluated by ELISA. IL-6 and IL-11 secretion were not observed from untreated WT or *Epim*$^{-/-}$ colonic myofibroblasts. **(A).** WT colonic myofibroblasts secrete 415, 512, and 597 pg/ml of IL-6 respectively ($p<0.05$ vs. no treatment) of IL-6 in response to increasing doses of IL-1β IL-6 secretion was not observed in response to treatment with 1.5 and 3 ng/ml of IL-1β treated *Epim*$^{-/-}$ colonic myofibroblasts. IL-6 secretion (16 pg/ml) was detected from *Epim*$^{-/-}$ myofibroblasts only in response to 100 ng/ml of IL-1β. **(B)** WT colonic myofibroblasts secrete 108 pg/ml of IL-11 in response to IL-1β ($p<0.05$ vs. no treatment). IL-11 secretion was not observed in IL-1 β treated *Epim*$^{-/-}$ colonic myofibroblasts.

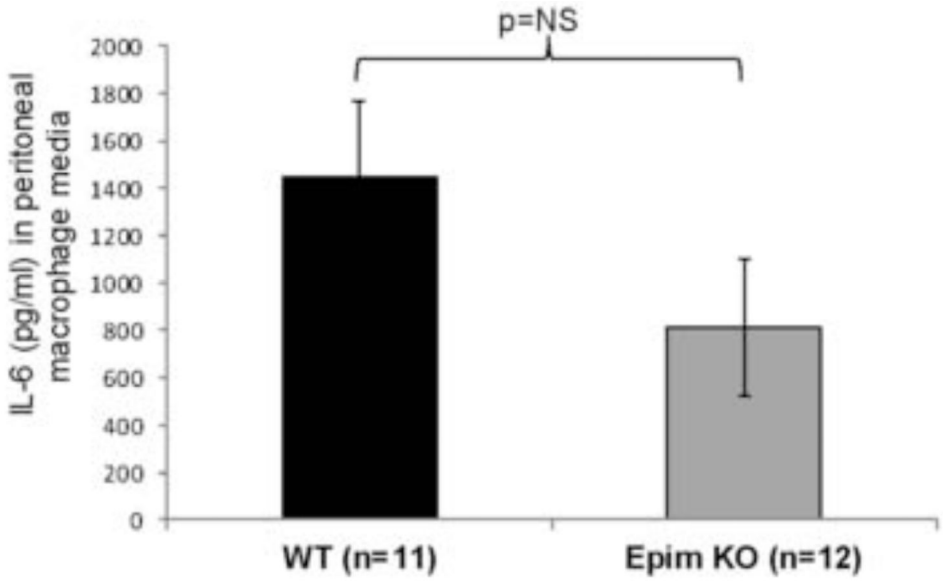

Figure 9. Effect of Epim deletion on peritoneal macrophage secretion of IL-6

Resident peritoneal macrophages were isolated by flushing the peritoneal cavity with cold PBS as described previously [16] from DSS treated WT and *Epim*$^{-/-}$ mice and plated (5×10^5 cells/well) in a 96 well plate as described in methods. After 24 hours, supernatants were collected for measurement of IL-6 secretion. ELISA (R&D) was performed per manufacturer's instructions. Results were expressed as pg of cytokine/ml. Despite a trend toward decreased secretion of IL-6, there was no significant difference in secretion of IL-6 from peritoneal macrophages of DSS treated WT versus *Epim*$^{-/-}$ mice.

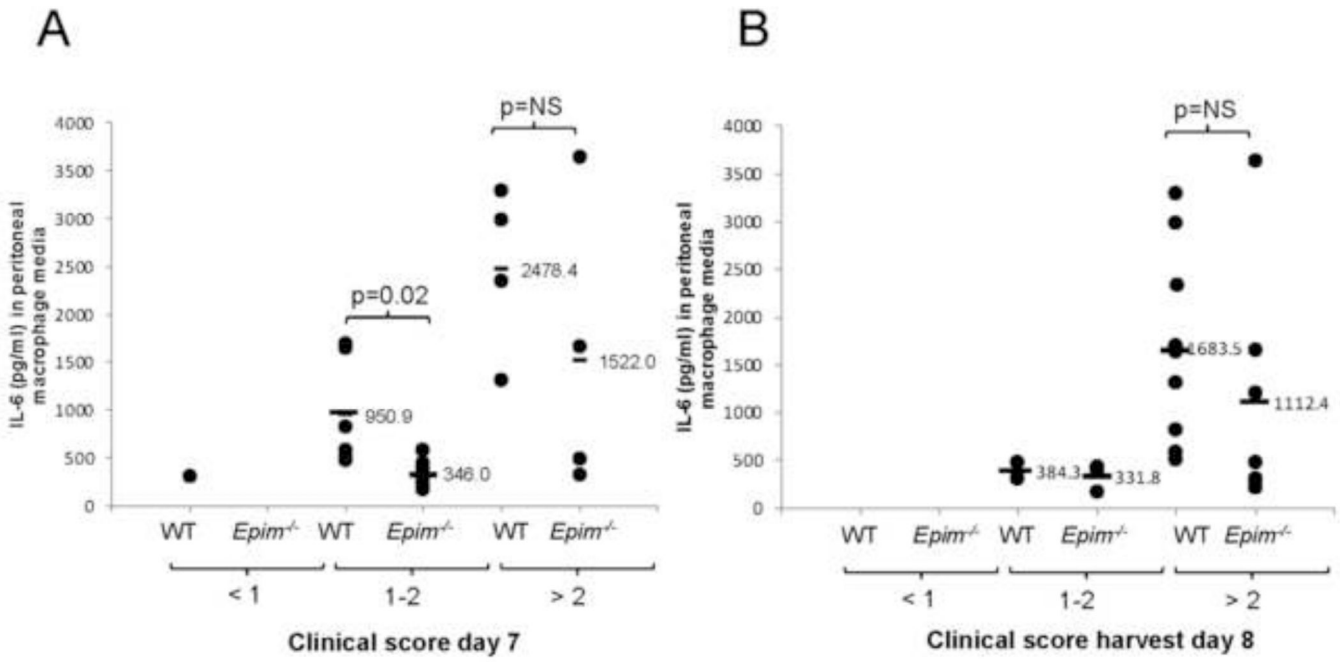

Figure 10. Peritoneal macrophage IL-6 secretion from WT and *Epim*$^{-/-}$ mice with similar clinical scores

Clinical scores were calculated for mice on day 7 (**A**) and on day 8 (harvest) (**B**) as described in methods, for WT (n=11) and *Epim*$^{-/-}$ (n=12) mice from which peritoneal macrophages had been harvested and IL-6 secretion examined. IL-6 (pg/ml) detected in media of each mouse (y-axis) was grouped according to clinical score (on the x-axis). **(A).** On day 7 of DSS, a distribution of clinical scores was observed such that peritoneal macrophage secretion within groups could be compared. A clinical score of 1-2 was observed in n=6 WT and n=7 *Epim*$^{-/-}$ mice. Secretion of IL-6 from *Epim*$^{-/-}$ vs. WT peritoneal macrophages in this group was decreased (346 pg/ml vs. 950.9 pg/ml, p=0.02). **(B)**. At the time of harvest, the majority of WT and *Epim*$^{-/-}$ mice had clinical scores > 2 and IL-6 secretion from WT and *Epim*$^{-/-}$ peritoneal macrophages was not significantly different.